

Development and Test of Nb₃Sn Cos-theta Magnets Based on RRP and PIT Strands

S. Feher, G. Ambrosio, N. Andreev, E. Barzi, B. Bordini, R. Bossert, R. Carcagno, V.S. Kashikhin, V.V. Kashikhin, M.J. Lamm, I. Novitski, Yu. Pischalnikov, C. Sylvester, M. Tartaglia, D. Turrioni, R. Yamada, A.V. Zlobin

Abstract—As part of the High Field Magnet program at Fermilab three cos(Θ) magnets - two mirror dipole magnets utilizing RRP cable and one dipole magnet utilizing PIT cable - have been designed, fabricated and tested recently. Both mirror magnets with RRP strands only reached ~50-60% of their estimated critical current limit. The PIT conductor based dipole however reached its critical current limit producing over 10 T magnetic field in the bore of the magnet. This paper describes the parameters of superconducting strands and cable, the details of magnet design and fabrication procedure, and reports the results.

Index Terms—Superconducting accelerator magnets, high field dipole, Nb₃Sn strands and cables, Powder-in-Tube technology

I. INTRODUCTION

FERMILAB is developing new generation high-field accelerator magnets exploring several different design and technological approaches. Recently tested magnets are build on a magnet design which is utilizing Nb₃Sn cos(Θ) coils and the wind-and-react technology. These magnets are single-bore dipole models which were developed based on the two-layer shell-type coils with a 43.5 mm bore and cold iron yoke [1]. Studies and optimization of magnet quench performance were done using magnet half-coils and magnetic mirror configuration [2]. The early dipole and mirror magnet models, using cable made with the Modified Jelly Roll (MJR) process, exhibited large degradation of magnet quench current relative to the expected short sample limit [3,4]. Extensive studies and results of special experiments indicated that the most probable explanation is conductor instability [5]-[10].

Using more stable Nb₃Sn strands with an effective filament size of ~50 microns utilizing the powder-in-tube (PIT) technology two cos(Θ) half-coils were fabricated and successfully tested in a mirror and dipole configurations last summer reaching 10T magnetic field in the bore of the magnet. These successful tests have proven an importance of the conductor stability for magnet quench performance

predicted by the stability analysis of Nb₃Sn strands and cables [5-6] and allowed to reach 10 T magnetic field. The mechanical structure developed for these magnets demonstrated reliable performance at fields up to 10 T.

The next step in the program was two folded: i) to increase the dipole field up to 11-12 T by using higher Jc strands, ii) to reproduce another successful 10 T dipole magnet utilizing the same stable PIT conductor. In order to achieve our first goal the magnet coil was modified for 0.7 mm strand without changing the coil layer width or magnet mechanical structure. High Jc strand with smaller (~80 μ m) sub-element size produced by Restack Rod Process (RRP) was used in order to mitigate the instability problems and increase the field. Three new half-coils based on this design were fabricated and two were tested in a magnetic mirror configuration. The second goal was achieved by fabricating a new dipole magnet using the same mechanical structure and the same PIT cable as it was used in the previous successful magnet.

This paper describes the parameters of both the Nb₃Sn RRP and PIT strand and cable, the details of coil design, magnetic mirror and the dipole fabrication procedures and reports the test results.

II. MAGNET DESIGN

The dipole model design is based on the two-layer shell-type coil with a 43.5 mm bore and cold vertically split iron yoke. The magnet coils are made of a keystone Rutherford-type cable with 28 (39) Nb₃Sn multi-filament strands, each 1 mm (0.7 mm) in diameter. The magnetic mirror configurations use the same mechanical structure with horizontally split yoke in which one of the two half-coils is replaced with the iron half-cylinder (magnetic mirror). Details of the magnet design and technology are described in [1,2].

A. Strand and Cable

Two types of strand were used: i) 0.7 mm strand produced by Oxford Superconductor Technologies (OST) using the RRP process, ii) 1.0 mm strand made by SMI (Netherlands) using the Powder-in-Tube process. Strand and cable parameters are shown in Table I. Rutherford-type cable from RRP strand for HFDM04 was manufactured at Lawrence Berkeley Laboratory (LBNL) in one step. The RRP cable for HFDM05 was fabricated in two steps: rectangular cable was made at LBNL and then the final keystone cable after

Manuscript received September 20, 2005.

This work was supported by the U.S. Department of Energy.

Authors are with the Fermi National Accelerator Laboratory (Fermilab), P.O. Box 500, Batavia, IL 60510 USA (phone: 630-840-2240; fax: 630-840-2383; e-mail: fehers@fnal.gov).

annealing was done at Fermilab. The cable for HFDA05 and HFDA06 was fabricated at Fermilab from PIT strand.

The cable insulation system for both PIT and RRP magnets consisted of 0.125 mm thick by 12.7 mm wide ceramic cloth, spiral wrapped around the cable. Two layers, each wrapped with 1mm gaps, offset so the 2nd layer was covering the gap in the 1st layer, were used on the HFDA05 coils. The 2nd layer was pre-impregnated with binder by the manufacturer. Non-organic liquid binder (CTD-1008) was also applied externally to the coil surfaces just before curing. Since pre-impregnated insulation was not available for the remaining PIT or RRP coils, a simpler system, consisting of a single layer with overlap was used. Dry ceramic cloth was wrapped with 40% overlap on HFDA06 coils and 30% overlap on HFDM04/5 coils, and binder was applied before curing. The overlap percentage was configured to create an azimuthal preload equivalent to the HFDA05 coils.

TABLE I
STRAND AND CABLE PARAMETERS

Parameter	Unit	PIT cable	RRP cable
Strand Diameter	mm	1.00	0.70
Number of sub-elements		127	54/61
Sub-element size	μm	50	80
Cu fraction	%	54	50
Cable Midthickness	mm	1.8	1.20*/1.24**
Cable Width	mm	14.24	14.36*/14.24**
Cable Keystone angle	deg	0.9	0.98*/0.91**
Cable Pitch Length	mm	110	111
Number of Strands		28	39

* HFDM04; ** HFDM05

B. Coil Design and Fabrication

Both PIT and RRP coils were wound using the coil-on-coil procedure, where the inner coil is wound and cured, ceramic inter-layer insulation is added, then the outer coil wound over the cured inner coil. Both coils are then cured together. Inner and outer coil layers are made from one continuous length of cable, eliminating the need for an inter-layer splice. End parts are made of aluminum bronze using water jet techniques.

Coil curing was done in a closed cavity mold manufactured to the nominal coil size at 150°C for ½ hour. To avoid damage at reaction temperatures, coil size is set during curing so that the maximum azimuthal pressure during reaction is less than 5 MPa. The final coil size was achieved during the reaction and impregnation processes and was nearly identical for both PIT and RRP coils.

Ground insulation, consisting of 3 layers of 0.125 mm ceramic sheet, was installed before reaction. Quench protection heaters were made of 0.025 mm thick by 12.7 mm wide stainless steel strips, installed on the outer coil exterior surface. PIT coils contained one strip per quadrant, while RRP coils contained two per quadrant. Each PIT coil pair was reacted at 655°C for 170 hours. The RRP coil reaction cycle consisted of three plateaus; 210°C for 100 hours, 400°C for 48 hours and 650°C for 50 hours. After reaction, each coil was impregnated with epoxy at 60°C, then cured at 125°C for 21 hours.

C. Magnetic Mirror Configuration HFDM04 and HFDM05

We used a horizontally split yoke approach for HFDM04 and HFDM05. Coil pre-compression was provided by mid-plane radial and azimuthal shims. Initially, end loading was not applied to either mirror. After the first test, HFDM05 was retested with a total end load of 7000 N applied.

D. Dipole Model HFDA06

The design and assembly procedure for HFDA06 was similar to that of our previous HFDA05 model [3]. The end plates and skin were bolted together. The coil pre-compression was provided by radial shims installed between the coil and coil-yoke spacer and additional radial shims installed between the spacer and the iron yoke near the coil mid-plane. The only difference between HFDA05 and HFDA06 was that the later had an end loading of 700 lbs per bullet.

Coils in HFDM04, HFDM05 and HFDA06 had voltage taps installed on the outer layer and on each block of the inner layer as well as across all Nb₃Sn/NbTi lead splices.

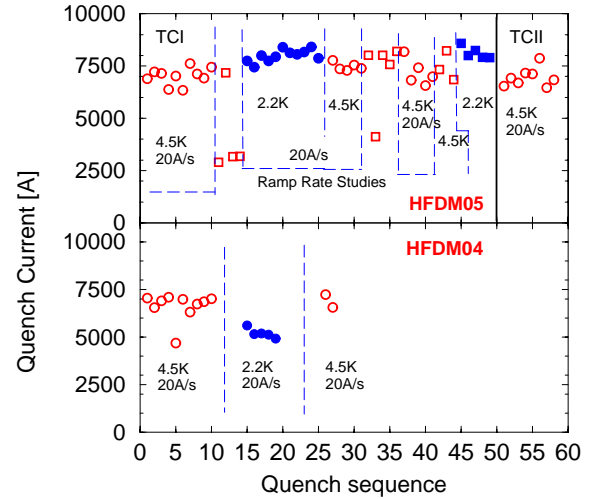


Fig. 1. HFDM04 and HFDM05 quench history.

III. TEST RESULTS

Magnetic mirror HFDM04, HFDM05 and dipole model HFDA06 were tested in the Vertical Magnet Test Facility at Fermilab in liquid helium bath between 2.2K-4.5K temperature range.

A. HFDM04 and HFDM05

The quench history of mirror magnet HFDM04 and HFDM05 is shown in Fig. 1. Both mirror magnets were tested at 4.5 and 2.2 K. Both magnets exhibited practically no training at 4.5 K. Quench current did not exceed 7 kA in HFDM04 and 8 kA in HFDM05. After training at 4.5 K the magnets were trained also at 2.2 K. In HFDM04 instead of increasing the quench currents decreased to ~5 kA. Quench behavior of HFDM05 at 2.2 K was quite the same as it was at 4.5 K with slightly increased quench current plateau. After increasing the temperature back to 4.5 K the quench currents

in both magnets went back to the same current range observed prior of quenching it at 2.2 K. In both magnets the resistive gauges mounted on the inner-layer coil surface and the resistive beam gauges installed in the mid-plane in the coil body showed elastic strain dependence as a function of the Lorentz force.

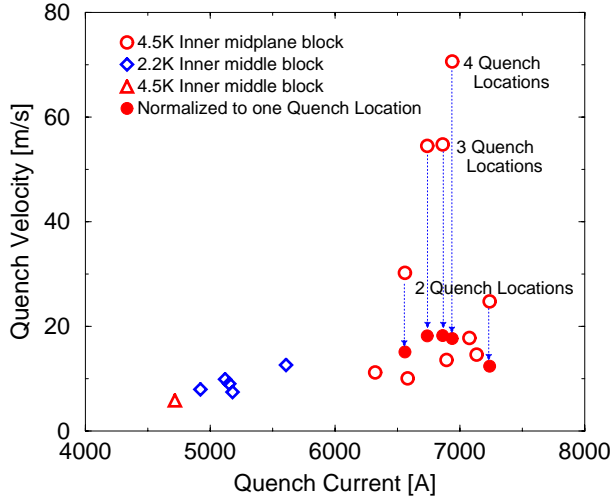


Fig.2. Quench propagation velocity based on voltage rise at the start of the quench.

After performing a thermal cycle and adjusting the magnet end support, HFDM05 was re-tested. However, the quench current values remained at the same level.

In HFDM04 all the training quenches but one at 4.5 K were located in the inner-layer mid-plane block. The 2.2 K quenches were in the inner-layer middle block region. In HFDM05 the training quenches at 4.5 K and 20 A/s ramp rates were located in the outer coil. Higher ramp rate quenches started both in the inner and outer coils almost simultaneously. The locations of training quenches at 2.2 K were alternated between the inner and outer coils. During the test many voltage spikes were detected in both magnets.

The measured RRR value for HFDM04 was 18 for the inner coil and 20 for the outer coil. The measured RRR value for HFDM05 was 55 for the inner coil and 30 for the outer coil.

We also observed that the voltage rise of a segment right after the quench started were not consistent with normal propagating zones (NPZ) initiated from a single location in the magnet. In Fig. 2. the quench velocity was plotted as a function of the quench current. The velocity was estimated by assuming a resistive rise due to double front of NPZ. One would expect low propagation velocities since the quenches occurred about half of the critical current limit of the conductor. On the other hand quantized jump of the quench velocity is only consistent with simultaneous quench starts at multiple locations. By dividing the quench velocity values with a whole number the obtained “normalized” new values line up with the rest of the quench velocity values. Multiple quench locations are consistent with an unstable conductor: thermal magnetic instability tend to propagate faster than a

quench and it could initiate quenches in multiple locations.

HFDM05 high ramp rate sensitivity was similar than the other dipole models which means that the 8 kA quench current plateau at low ramp rates is clearly not related to AC losses.

Low quench current values, erratic quench behavior, intensive voltage spikes and multiple quench locations indicate that the magnets were likely to be limited by conductor instabilities.

B. HFDA06

The quench training of dipole model HFDA05 is shown in Fig.3. and compared with that of HFDA05. The first training quench of HFDA06 at 4.5 K was close to 15.0 kA. It took only 10 quenches and the magnet reached a stable current plateau at 16.4 kA. In thermal cycle II the 4.5 K magnet training was short, the third quench was already at the previous quench current plateau. To expose the magnet to higher force level the magnet was cooled down to 2.2 K. It took only four quenches to reach the quench plateau of 17.6 kA. Warming up the magnet back to 4.5 K the magnet quench current did not change relative to its previous 4.5 K quench current plateau value.

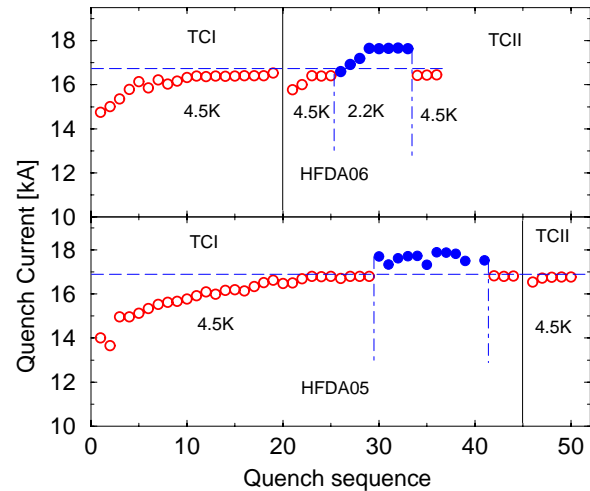


Fig.3. HFDA06 and HFDA05 quench training.

In both thermal cycles all the training quenches occurred in the inner-layer pole and middle block of half-coil 14, however all of the quenches at the plateau were in coil 15. Training data show that the magnet has reached its short sample limit at 4.5 K. The maximum field in the bore (coil) at 4.5 K was 9.6 T (10.0 T) and at 2.2 K was 10.2 T (10.6 T).

HFDA06 quench training was shorter than that of HFDA05 and the new magnet 2.2 quench behavior was more stable. We also noticed that the quench current value of HFDA06 at 20A/sec ramp rate was about 2% less than that of HFDA05. However, from ramp rate dependence studies (see Fig. 5.) extrapolating quench current values to 0 A/sec ramp rates one can conclude that the critical current limits of the two magnets are almost identical.

The dependence of magnet quench current vs. temperature for HFDA06 presented in Fig. 4. also confirmed that the

magnet reached its critical current limit. HFDA06 temperature dependence shows excellent agreement with HFDA05 data.

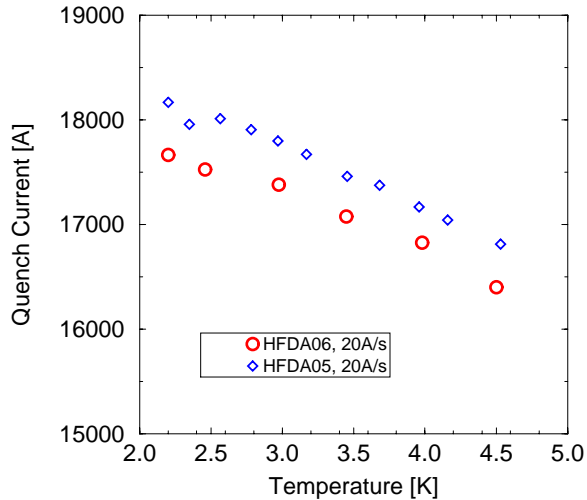


Fig. 4. Temperature dependence of HFDA05 and HFDA06 quench current.

Quench current ramp rate dependences at 4.5 K and at 2.2 of HFDA06 is plotted and compared to previously measured HFDA05 data in Fig. 5. As one would expect for a magnet which is not limited at low ramp rates the quench current decreases with increasing ramp rate and follows a continuous function. At ramp rates higher than 200 A/s the quench current drops dramatically and practically does not change with the current ramp rate. HFDA06 quench locations up to 150 A/s occurred in the inner coil, however all of the quench location at higher than 150 A/s ramp rates were in the outer coil. These behaviors indicate that for high ramp rate quenches the magnet is limited by high losses and insufficient coil cooling conditions especially in the second layer which has no direct contact with liquid helium.

At less than 100A/s ramp rates the shape of the ramp rate dependence for the two magnets is different. Steeper drop of the ramp rate for HFDA06 is an indication that the current distribution in the magnet is uneven. We noticed that by pre-cycling the magnet between 0–15kA then ramping with the same ramp rate to quench the quench current increased by ~2%.

IV. CONCLUSION

In order to reach higher fields two high Jc RRP coils were tested in two magnetic mirror configurations. Both magnets exhibited poor quench performance due to conductor instabilities. Using stable PIT conductor another 1m long dipole was built and successfully tested reaching over 10 T magnetic field. These tests demonstrated the importance of the conductor stability in building high field accelerator magnets and also proved that once the conductor is stable the magnet technology has been developed to build reliably up to 10 T magnets.

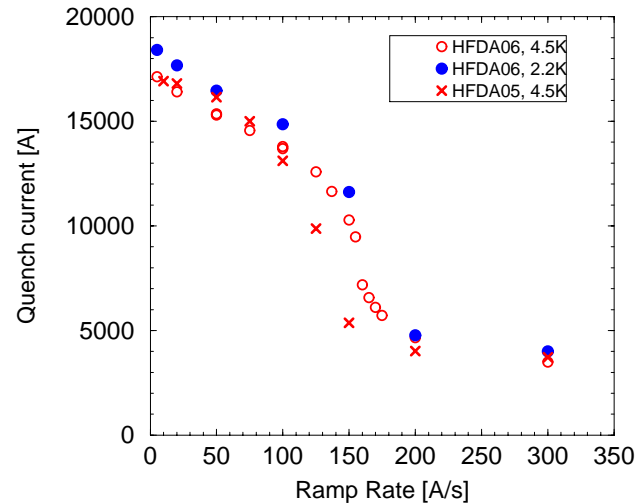


Fig. 5. Ramp rate dependence of magnet quench current.

ACKNOWLEDGMENT

The authors thank the staff of Fermilab's Technical Division for their contribution to this effort.

REFERENCES

- [1] G. Ambrosio et al., "Development of the 11 T Nb₃Sn Dipole Model at Fermilab", IEEE Trans. on Applied Superconductivity, v. 10, No. 1, March 2000, p.298.
- [2] D.R. Chichili et al., "Design, Fabrication and Testing of Nb₃Sn Shell Type Coils in Mirror Magnet Configuration", CEC/ICMC 2003, Alaska, September 22-25 2003.
- [3] N. Andreev et al., "Development and test of single-bore cos-theta Nb₃Sn dipole models with cold iron yoke", MT-17, IEEE Trans. on Applied Superconductivity, v. 12, No. 1, p. 332, March 2002.
- [4] S. Feher et al., "Test Results of Shell-type Nb₃Sn Dipole Coils", MT-18, Japan, October 2003.
- [5] V.V. Kashikhin, A.V. Zlobin, "Magnetic Instabilities in Nb₃Sn Strands", Fermilab Technical note, TD-03-032, July 21, 2003.
- [6] V.V. Kashikhin, A.V. Zlobin, "Magnetic instabilities in Nb₃Sn strands and Cables", IEEE Transactions on Applied Superconductivity, Volume 15, Issue 2, June 2005 Page(s):1621 - 1624
- [7] E. Barzi et al., "Instabilities in Transport Current Measurements of Nb₃Sn Strands", IEEE Transactions on Applied Superconductivity, Volume 15, Issue 2, June 2005 Page(s):3364 - 3367
- [8] G. Ambrosio et al., "Critical Current and Instability Threshold Measurement of Nb₃Sn Cables for High Field Accelerator Magnets", IEEE Transactions on Applied Superconductivity, Volume 15, Issue 2, June 2005 Page(s):1545 - 1549
- [9] E. Barzi et al., "Study of Nb₃Sn Cable Stability at Self-field Using a SC Transformer", IEEE Transactions on Applied Superconductivity, Volume 15, Issue 2, June 2005 Page(s):1537 - 1540
- [10] S. Feher et al., "Cable Testing for Fermilab's High Field Magnets Using Small Racetrack Coils", IEEE Transactions on Applied Superconductivity, Volume 15, Issue 2, June 2005 Page(s):1550 - 1553
- [11] D.R. Chichili et al., "Fabrication of Nb₃Sn Shell-Type Coils with Pre-Preg Ceramic Insulation", CEC/ICMC 2003, Alaska, September 22-25, 2003.
- [12] E. Barzi et al., "Sensitivity of Nb₃Sn Rutherford-type cables to transverse pressure", IEEE Transactions on Applied Superconductivity, Volume 15, Issue 2, June 2005 Page(s):1541 - 1544